Available online at www.eccomasproceedia.org
Eccomas Proceedia COMPDYN (2025) 6106-6117

ECCOMAS
Proceedia

COMPDYN 2025
10th ECCOMAS Thematic Conference on
Computational Methods in Structural Dynamics and Earthquake Engineering
M. Papadrakakis, M. Fragiadakis (eds.)
Rhodes Island, Greece, 15-18 June 2025

NON-LINEAR SOIL BEHAVIOR AND LIQUEFACTION SUSCEPTIBILITY IN LEBANON: A 1D NUMERICAL APPROACH

Hiba Labaki[1, 2], Etienne Bertrand[3,4], Luis Fabian Bonilla[3,4], Marleine Brax[2], and Muhsin Elie Rahhal[1]

[1]Saint Joseph University of Beirut - Faculty of Engineering, Beirut, Lebanon
hiba.labaki@net.usj.edu.lb
muhsin.rahal@usj.edu.lb

[2]CNRS-L, National Center for Geophysics, Bhannes, Lebanon
brax@cnrs.edu.lb

[3]Gustave Eiffel University, GERS-SRO, 14-20 bvd Newton, 77420 Champs-sur-Marne, France
[4]Paris Cité University, IPGP, 1 rue Jussieu, 75005 Paris, France
etienne.bertrand@univ-eiffel.fr
luis-fabian.bonilla-hidalgo@univ-eiffel.fr

Abstract

This study utilizes non-linear 1D simulation as a tool to explore the non-linear soil response and liquefaction susceptibility in Lebanon. Assessing seismic hazard in Lebanon is crucial due to its history of significant earthquakes, highlighting the need to understand non-linear soil behavior, particularly for long return periods. The analysis integrates the liquefaction front model, which captures pore pressure generation and dilatant soil behavior.
In the absence of laboratory data, Standard Penetration Test (SPT) data is used to derive Liquefaction Resistance Curves (LRCs) by means of empirical methods. These LRCs are then inverted using the Neighborhood Algorithm (NA) to extract the dilatancy parameters necessary for simulating soil behavior under cyclic loading. Additionally, the study analyzes non-linear soil behavior under a strong motion in the finite-difference code NOAH (NOn-linear Anelastic Hysteretic) to evaluate its response. This comprehensive approach offers a valuable framework for evaluating site-specific non-linear soil behavior and liquefaction potential in Lebanon, contributing to the region's seismic hazard assessment.

Keywords: Liquefaction Susceptibility in Lebanon, 1D Non-linear Numerical Modeling, Seismic Hazard.

ISSN:2623-3347
Peer-review under responsibility of the organizing committee of COMPDYN 2025.
doi: 10.7712/120125.12875.25652

1 INTRODUCTION

Soil liquefaction is a critical phenomenon that poses significant risks to infrastructure and urban environments during seismic events. This study focuses on studying soil liquefaction in the eastern suburbs of Beirut, Lebanon, with an emphasis on investigating the non-linear behavior of soil under cyclic loading. Since soils exhibit complex responses — such as stiffness degradation, hysteresis, and pore pressure buildup — advanced numerical simulations are essential for accurate seismic hazard assessments.

This research employs the finite-difference code NOAH (NOn-linear Anelastic Hysteretic) to perform 1D non-linear soil simulations. NOAH integrates the multishear mechanism model [1] to capture hysteretic stress-strain behavior and the liquefaction front model [2] to simulate cyclic mobility of cohesionless soils.

A major challenge in using advanced constitutive models is the calibration of the parameters. NOAH requires physically meaningful input parameters such as shear wave velocity (Vs), density (ρ), friction angle (φ), and cohesion (c). Additionally, the liquefaction front model involves five dilatancy parameters that influence pore pressure evolution but are difficult to measure directly. Laboratory tests for these parameters are limited and expensive, and sample disturbances can affect their reliability.

To overcome these challenges, previous studies have explored alternative calibration methods such as Janusz *et al.* [3, 4] that used Cone Penetration Test (CPT) data with inversion techniques for parameter estimation. Inspired by this approach, the present study utilizes Standard Penetration Test (SPT) data for parameter estimation.

Numerical simulations are a useful tool to assess the impact of non-linear soil behavior and cyclic mobility for the selected site. Despite the limitations of a 1D approximation, these simulations offer valuable insights into seismic risks and soil response under cyclic loading. In this paper, we will present the methodology employed in our study, followed by the case study analysis. Finally, we will discuss the results and conclusions drawn from our findings.

2 METHODOLOGY

2.1 Liquefaction front model definition

Initially implemented by Towhata and Ishihara [1] and later expanded by Iai *et al.* [2], this approach considers both the cyclic mobility and dilatancy of sands. The model is based on the correlation between pore pressure buildup and cumulative shear work under cyclic loading conditions [1].

The model is an empirical approach that models the reduction of effective confining stress due to the increase in pore water pressure, up to reaching the transformation (dilatancy) line or the failure (liquefaction) line (Figure 1). Defined respectively by φ_p ($m_2 = \sin\varphi_p$) and φ ($m_1 = \sin\varphi$), these lines characterize the liquefaction front via the state parameter S ($p'/p'_o = \sigma'_m/\sigma'_{mo}$), which represents the ratio of the mean effective stress σ'_m to the initial mean effective stress σ'_{mo}, ranging from 0 (liquefaction) to 1 (no pore pressure generation). Further explanation of this model is provided through an example of a simulated stress-controlled experiment (Figure 2), where the gradual decrease in effective confining pressure as cyclic loading progresses illustrates the development of pore pressure over time. As cyclic shear stress τ is applied, the stress path moves toward the failure line, demonstrating the progressive weakening of the soil structure due to excess pore pressure generation.

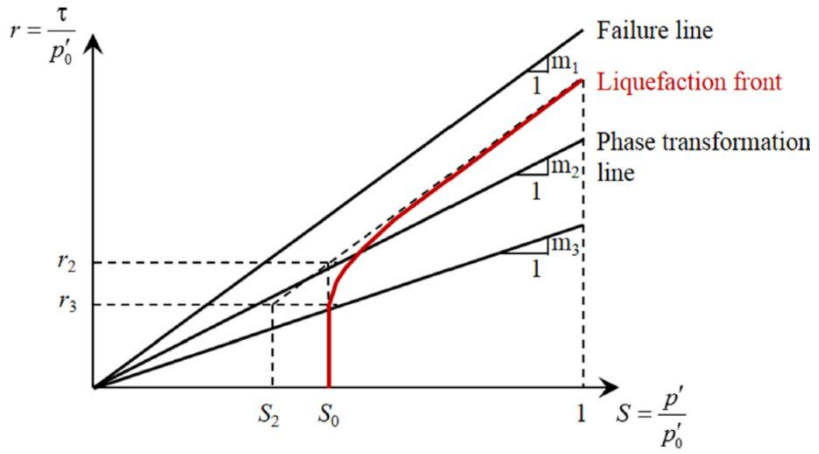

Figure 1: Liquefaction front model representation.

The state parameter S is a function of the cumulative shear work w, as shown in Equations (1) and (2):

$$S = (0.4 - S_1)\left(\frac{w_1}{w}\right)^{p_2} + S_1 \quad \text{if } w \geq w_1 \qquad (1)$$

$$S = 1 - 0.6\left(\frac{w}{w_1}\right)^{p_1} \quad \text{if } w < w_1 \qquad (2)$$

To characterize layers prone to cyclic mobility and liquefaction, it is essential to define five dilatancy parameters that describe how excess pore pressure develops in the liquefaction front model [2].

The first parameter S_1 will have a small positive value (0.01), to ensure numerical stability, since S cannot be zero.

The four other dilatancy parameters shape the function governing pore pressure evolution over time and are illustrated in Figure 2. The initial dilatancy parameter, p_1, influences the speed of pore pressure buildup during the early deformation stage, while the final dilatancy parameter, p_2, affects the terminal phase. The overall dilatancy parameter, w_1, determines the general curve shape. Lower values of p_1 and w_1 lead to a faster pore pressure increase, whereas a lower p_2 slows the rise. The threshold limit, c_1, defines the shear work level at which pore pressure starts to build up.

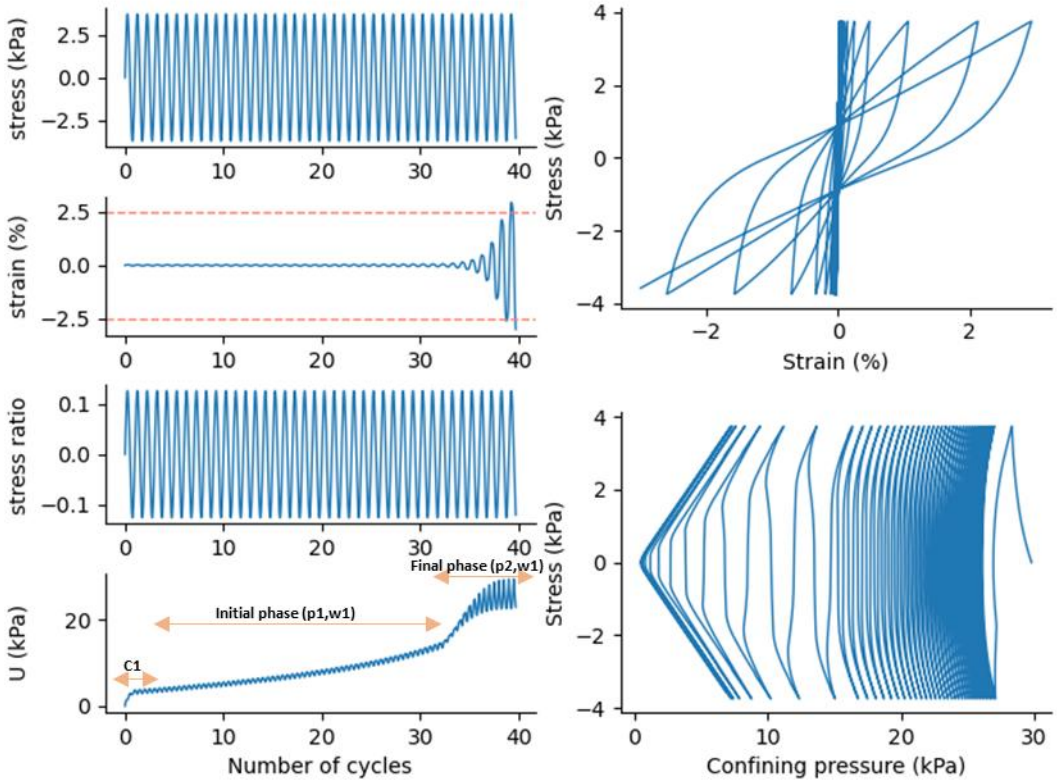

Figure 2: Results of stress, strain, stress ratio, and pore water pressure vs. number of cycles (left panel) and stress-strain and stress-confining pressure relationships (right panel) for an example of a simulated stress-controlled experiment.

2.2 Inversion procedure for dilatancy parameters via Neighborhood Algorithm

We estimate the dilatancy parameters following the inversion procedure of Janusz *et al.* [3, 4]. The Liquefaction Resistance Curve (LRC) which is the relationship between the Cyclic Stress Ratio (CSR) and the number of cycles (N), is estimated by the cyclic resistance ratio (CRR7.5), from SPT data, and the Magnitude Scaling Factor (MSF) following Boulanger and Idriss [5]. CRR7.5 represents the cyclic stress ratio (CSR) needed to trigger liquefaction during 15 uniform loading cycles, equivalent to the impact of a magnitude 7.5 earthquake. A high CSR, associated with strong and prolonged earthquakes, requires fewer cycles to induce liquefaction, while a low CSR demands more cycles. The Liquefaction Resistance Curve (LRC) formula can be obtained by the Equations (3) and (4).

$$CSR = \tau / \sigma'_{mo} = CRR_{7.5} \cdot MSF \quad (3)$$

$$N = \frac{15}{MSF^{\frac{1}{0.337}}} \quad (4)$$

Where τ represents the Cyclic Shear Stress and σ'_{mo} is the initial mean effective stress.

After defining the Liquefaction Resistance Curve (LRC) for the liquefiable layer, we apply the inversion procedure using the Neighborhood Algorithm [6] to determine the four dilatancy parameters that best reproduce the LRC. In the Neighborhood Algorithm, several parameters govern the sampling of the model space (Table 1). Initially, the model space is divided into a specified number of cells (ni) for the first iteration. During subsequent iterations, the nr cells with the lowest misfit are subdivided into ns/nr new cells, where ns represents the sample size

for all other iterations. This process continues until the maximum number of iterations (n) is reached. Given the often non-unique nature of the inversion results for dilatancy parameters, the algorithm must balance between exploring local minima and maintaining computational efficiency.

A stress-controlled experiment is simulated for each CSR value in simple shear mode, using the liquefaction front model from Iai *et al.* [2].

The applied stress σ_{xy} in the experiment is computed as a function of the number of cycles (N), the cyclic stress ratio (CSR), and the initial mean effective stress (σ'_{mo}), with time step dt (Equation 5):

$$\sigma_{xy} = \sin[2.\pi.dt.(N-1)]\,.CSR.\sigma'_{mo} \qquad (5)$$

The goal is to identify models where liquefaction occurs at CSR values and cycle counts comparable to those on the LRC curve. Liquefaction is assumed to begin when the strain reaches 2.5% (or 5% double amplitude) [7] (example shown in Figure 2).

The misfit between the model and empirical data is calculated using Equation 6, where n is the number of samples in the LRC curve:

$$misfit = \sum_{k=1}^{n} \left(\frac{data_k - model_k}{model_k}\right)^2 \qquad (6)$$

In cases where the 2.5% strain threshold is not reached for low CSR values due to insufficient stress, the lowest CSR values are excluded from the analysis.

2.3 1D numerical modeling in NOAH

The 1-D finite-difference code NOAH [8, 9] is utilized to model wave propagation in water-saturated non-linear media subjected to vertically incident, horizontally polarized shear (SH) waves.

It can simulate both linear viscoelastic and non-linear materials, performing analyses under total stress conditions (without excess pore pressure generation) and effective stress conditions (accounting for excess pore pressure generation).

For effective stress modeling, NOAH incorporates the liquefaction front model [2] to represent the cyclic mobility of dilatant sands under undrained conditions.

3 CASE STUDY

This study focuses on a site located in the eastern suburbs of Beirut, Lebanon, near the Beirut River.

From a geological perspective, the site consists of Quaternary formations, specifically sandy alluvium overlying Cretaceous formations. The Quaternary deposits include various soil types and unconsolidated materials covering the exposed rock formations. A shallow groundwater table is present at approximately 2 meters' depth, which aligns closely with the sea level.

Standard Penetration Tests (SPT) were conducted every 1.5 meters of depth. The site is composed of four distinct layers: fill material (between 0 m and 2 m), sand (between 2 m and 16.5 m), sandy clay (between 16.5 m and 28 m), and a deeper sand layer (between 28 m and 45 m). Some of the sandy layers, classified as liquefiable with low N-SPT values, are primarily observed between the surface and 15 meters. Key geotechnical parameters, such as shear wave velocity, internal friction angle, and porosity, were determined using empirical models and laboratory tests.

Lebanon is situated along the Levant Fault System, a ~1,200 km-long transform fault extending from the Red Sea seafloor spreading zone to the Taurus region in southern Turkey. This fault system is a major tectonic feature responsible for much of the seismic activity in the Eastern

Mediterranean region. Historical earthquakes, such as the catastrophic 551 AD earthquake, highlight the exposure of Lebanon to significant seismic events and the lack of strong motion recordings poses challenges for site-specific seismic analysis.
Due to the absence of strong motion data in Lebanon, the SM502 recording from the European Strong Motion Database was selected as the input motion. This signal corresponds to the Mw 6.5 Island Earthquake of June 17, 2000, which had a peak ground acceleration of 0.529 g at a station located 8.4 km from the epicenter. The response spectra of this event closely match the estimated elastic response spectrum of the 551 AD earthquake [10], making it a suitable input for the site response analysis.

4 ANALYSIS AND DISCUSSION

4.1 Choice of the optimal number of iterations for the inversion

The Neighborhood Algorithm (NA) [6] is defined by the number of iterations *ns, nr, ni, n,* required to achieve optimal inversion results, ensuring the best misfit while maintaining an acceptable computation time. To determine these appropriate values, multiple tests were conducted on the liquefiable layers 2 and 4. These tests were carried out to refine the parameter selection process before applying it to all five layers prone to liquefaction (Layers 2, 4, 5, 6, and 7). The objective was to determine the optimal values of the four dilatancy parameters for each layer, minimizing the misfit while keeping computational costs within reasonable limits.
The results indicated that the optimal values are those presented in Table 1. Using lower values than those adopted results in faster computation times; however, the algorithm lacks sufficient exploration.
Conversely, increasing the values beyond those in Table 1 introduces a time constraint without any significant improvement in misfit or exploration.

Number of iterations	Value
ns	40
nr	20
ni	40
n	200

Table 1: Parameters adopted in this study for the inversion in the Neighborhood Algorithm.

4.2 Inversion results for dilatancy parameters via Neighborhood Algorithm

In this study, the Liquefaction Resistance Curve was constructed using 12 Magnitude Scaling Factors (MSF) values distributed between 0.4 and 1.8.
To reproduce this LRC, the set of the four dilatancy parameters (p_1, p_2, w_1, and c_1) was inverted jointly based on the Neighborhood algorithm [6]. After running the inversion process with the input parameters defined in Table 1 and the search range input parameters defined in Table 2 for all five liquefiable layers, we confirmed that the inversion method is non-unique. The results shown in Figure 3, yielded not only the dilatancy parameters corresponding to a minimum misfit but also those associated with an acceptable misfit (for example less than 0.5).

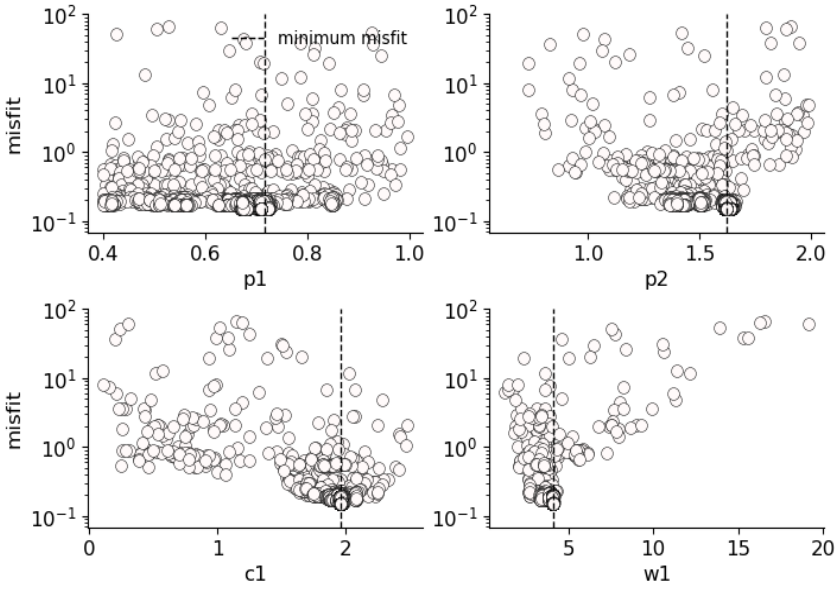

Figure 3: Sets of dilatancy parameters during one inversion run for layer 2.

The Liquefaction Resistance Curves (LRC) generated from a single inversion run, along with their corresponding misfit for layer 2, are presented in Figure 4. Additionally, the Liquefaction Resistance Curve obtained from the Standard Penetration Test (SPT) is represented by the curve with circular markers for comparison.

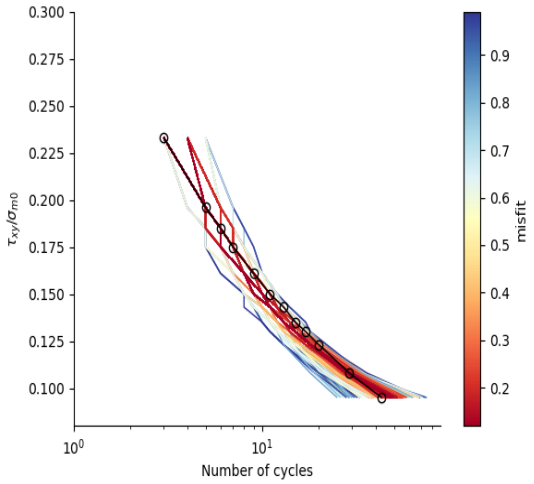

Figure 4: Liquefaction Resistance Curve (LRC) obtained from the SPT test for layer 2 (represented by circular markers) compared to LRCs from a single inversion run, with misfit indicated by color.

The values obtained after inversion for the lowest misfit in each liquefiable layer are summarized in Table 2. Additionally, the table includes the search limits for the model space tested across various search ranges to validate the results reported by Iai *et al*. [2].

	Layer 2	Layer 4	Layer 5	Layer 6	Layer 7	Search Range
p1	0.564	0.432	0.453	0.414	0.409	0.4 - 1.0
p2	1.936	1.941	1.935	1.413	1.943	0.6 - 2.0
c1	2.003	2.19	2.017	2.004	2.47	0.1 – 2.5
w1	3.96	4.79	4.521	3.433	5.39	1 – 20.0
Lowest Misfit	0.12	0.168	0.149	0.157	0.215	
Mid-Depth (m)	2.75	6.25	8.25	9.75	11.25	
Layer thickness (m)	1.5	2.5	1.5	1.5	1.5	

Table 2: Results of the lowest misfit set of dilatancy parameters for the liquefiable layers with their location and thickness and the model space search ranges adopted in the inversion.

4.3 Non-linearity results in NOAH

The obtained dilatancy parameters values are implemented in NOAH to investigate the impact of non-linear soil behavior and assess the potential for cyclic mobility at the selected site.

To account for the free surface effect, we divided the recorded input ground motion by two and applied an elastic boundary condition at the base of the soil column.

We simulated 1D wave propagation at the selected site using three different soil behavior models to evaluate the effects of non-linearity and liquefaction on the soil response. The first model is purely linear, which assumes elastic behavior. The second model is non-linear with a total stress analysis applied to the entire soil column. The third model is non-linear with an effective stress analysis, where pore pressure effects are only considered in the liquefiable layers, while all other non-linear layers are modeled using a total stress approach, where excess pore pressure is not computed.

Figure 5 presents the surface acceleration time histories for various soil behavior models and the amplification as a function of frequency. The linear model exhibits the highest acceleration amplitudes (5 m/s^2), indicating minimal energy dissipation due to the absence of non-linear effects. In contrast, the non-linear total stress model and the non-linear effective stress model show a reduction in peak acceleration values (around 2.5 m/s^2), highlighting the impact of soil non-linearity and energy dissipation mechanisms. The effective stress model, which accounts for pore pressure generation in liquefiable layers, exhibits a change in frequency content during the later phases, a typical nonlinear soil behavior response associated to the cyclic mobility within the soil.

For the frequency-dependent amplification for the three models, the linear model shows the highest amplification, particularly around 1 Hz. As for the non-linear models, the soil response impacts site resonance, shifting fundamental frequencies toward lower values due to shear modulus degradation under large strains. In addition, the effective stress analysis shows an amplification peak around 1 Hz, attributed to the cyclic mobility within the soil. Another consequence of cyclic mobility is the progressive attenuation of high frequencies once it starts, becoming noticeable beyond 3 Hz, where the effective stress model curve drops below that of the total stress model.

This analysis shows that taking only the linear behavior gives conservative results especially at high frequencies. This highlights the necessity of incorporating non-linear effective stress models in seismic site response studies to capture the complex behavior of liquefiable soils under cyclic loading.

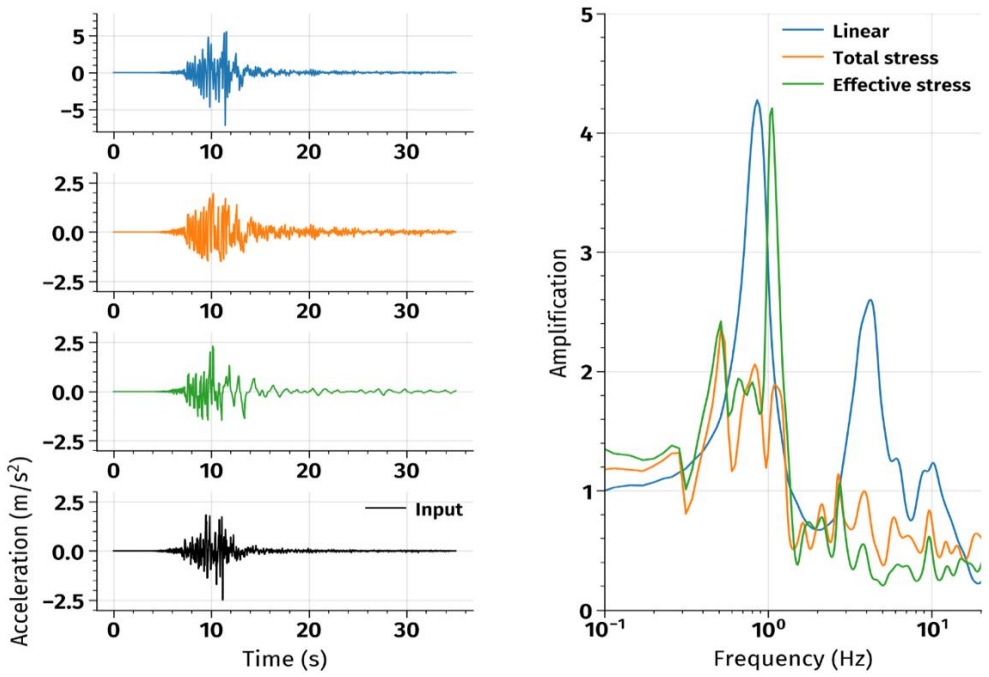

Figure 5: Acceleration time histories for the input motion and for the different soil behavior models, along with their Fast Fourier Transfer function.

The strain-depth profile in Figure 6 illustrates the impact of different soil behavior models on deformation. Non-linear analyses (effective stress and total stress) exhibit higher strain values compared to linear models, highlighting the importance of accounting for non-linear soil behavior under seismic loading. At the liquefiable layer 2 (between 2 and 3.5 meters), strain values are significantly elevated (around 10%), indicating significant cyclic mobility of the dilatant soil and possible liquefaction in this zone. This is highlighted in Figure 7, which shows that at a depth of 2.8 meters, the excess pore pressure nearly equals the initial confining pressure. Additionally, the stress-strain loops at this depth exhibit pronounced hysteresis with progressive softening, characterized by increasing strain amplitude and a reduction in stiffness. As for the layers between 5 and 12 meters, they exhibit lower strain values. In Figure 7, at a depth of 9 meters, although there is an increase in pore pressure, it does not reach the initial confining pressure, and the stress-strain loops display less pronounced hysteresis and more stable cyclic behavior. These results demonstrate that susceptibility to liquefaction and cyclic mobility decreases with depth.

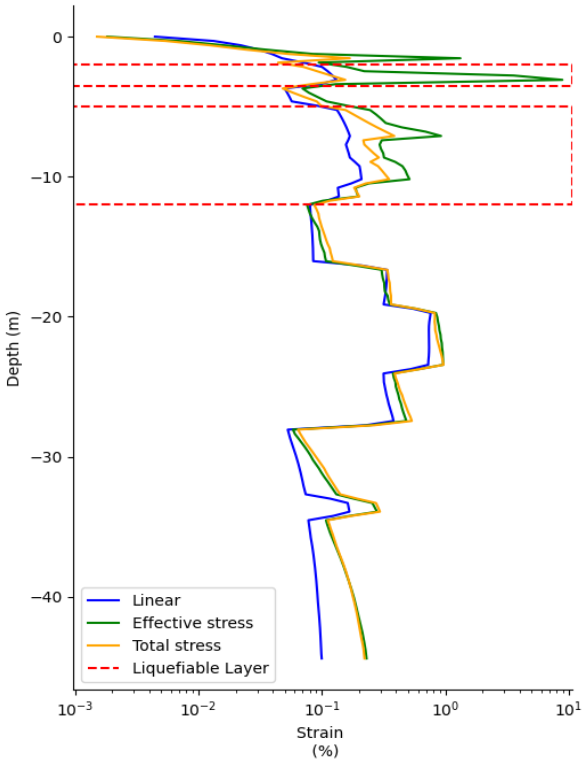

Figure 6: Strain vs. depth for the three soil behavior models.

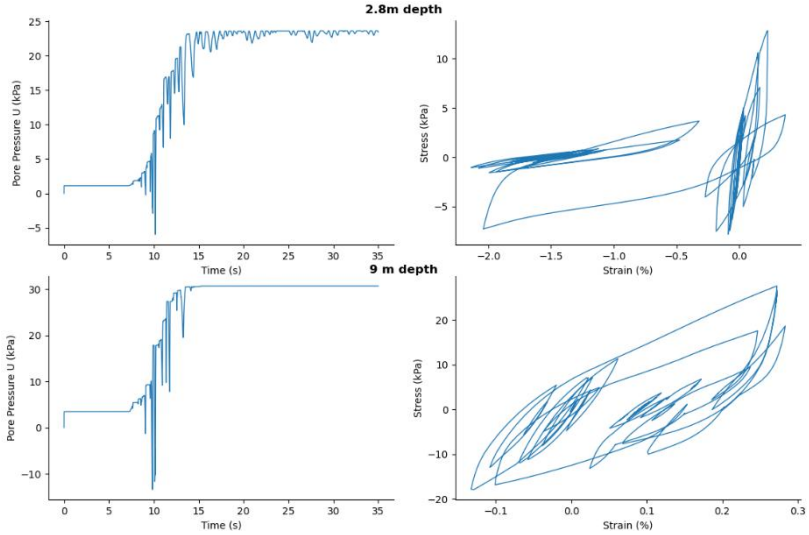

Figure 7: Pore pressure time history (left panel) and stress-strain relationship (right panel) results from a 1D non-linear effective stress simulation at depths of 2.8 m (upper panel) and 9 m (lower panel).

5 CONCLUSION

This study provides a comprehensive assessment of soil liquefaction susceptibility in the eastern suburbs of Beirut through advanced numerical modeling. Based on the liquefaction front model, an inversion using the Neighborhood Algorithm was performed to estimate dilatancy parameters from SPT data. Although the inversion process is non-unique, this approach remains valuable as it enables the identification of reasonable dilatancy parameters through a computationally efficient and cost-effective method, particularly in the absence of laboratory tests.

After implementing the estimated dilatancy parameters in the 1D finite-difference code NOAH, the results highlight the importance of considering soil non-linearity in seismic response analyses. While linear models tend to be conservative, non-linear modeling captures the true complexity of soil behavior under cyclic loading. Additionally, the results revealed that shallow depths exhibit a high liquefaction potential, with numerical simulations providing a more detailed understanding of the cyclic mobility of each soil layer. For instance, layer two (a shallow-depth layer) showed significantly higher strain values and pore pressure buildup compared to other liquefiable layers. This approach enhances the accuracy of liquefaction assessment by offering a clearer and more precise representation of soil behavior under cyclic loading, compared to deterministic and probabilistic methods. Consequently, this method proves to be an effective tool for improving liquefaction hazard evaluation in Lebanon.

Future research should focus on assessing the sensitivity of the inversion process to a range of acceptable misfits, rather than solely the lowest one, to evaluate their influence on non-linear behavior. Furthermore, studying the non-linear response under different input motions will help quantify the variability in liquefaction susceptibility and improve its assessment.

REFERENCES

[1] I. Towhata, K. Ishihara, Modeling soil behavior under principal axes rotation. *Proceedings of the 5th International Conference on Numerical Methods in Geomechanics*, 523–530, Nagoya, April 1–5, 1985.

[2] S. Iai, Y. Matsunaga, T. Kameoka, Parameter identification for a cyclic mobility model. *Report of the Port and Harbour Research Institute*, 29(4), 57–183, 1990.

[3] P. Janusz, P. Bergamo, L. F. Bonilla, F. Panzera, D. Roten, K. Loviknes, D. Fäh, Multistep procedure for estimating non-linear soil response in low seismicity areas—a case study of Lucerne, Switzerland. *Geophysical Journal International*, 239(2), 1133–1154, 2024.

[4] P. Janusz, L.F. Bonilla, D. Fäh, URBASIS Deliverable: A case study on non-linear soil response in urban areas. *ETH Zurich*, 2022.

[5] R.W. Boulanger, I.M. Idriss, CPT and SPT based liquefaction triggering procedures. *Center for Geotechnical Modeling, Department of Civil and Environmental Engineering, University of California*, Davis, 2014.

[6] M. Sambridge, Geophysical inversion with a neighbourhood algorithm—I. Searching a parameter space. *Geophysical Journal International*, 138(2), 479–494, 1999

[7] M.E. Rahhal, G. Lefebvre, Understanding the effect of static driving shear stress on the liquefaction resistance of medium dense sand. *Soil Dynamics and Earthquake Engineering*, 8, 397–404, 2001

[8] L.F. Bonilla, NOAH: User's Manual, Institute for Crustal Studies. *University of California, Santa Barbara, USA, Institut de Radioprotection et de Sureté Nucléaire*, France, 2001.

[9] L.F. Bonilla, R. Archuleta, D. Lavallée, Hysteretic and dilatant behavior of cohesionless soils and their effects on non-linear site response: field data observations and modeling. *Bulletin of the Seismological Society of America*, 95, 2373–2395, 2005.

[10] M. Brax, H. Labaki, P.-Y. Bard, Beirut Urban Resilience Master Plan (Phase II) Data Scoping; Seismic, and Tsunami Hazard Assessments: Deliverable 6 Spectral Accelerations Per Zone: Deterministic Approach. *National Council for Scientific Research. Report submitted to the World Bank*, 2020.